Journal of Materials Chemistry C

Accepted Manuscript

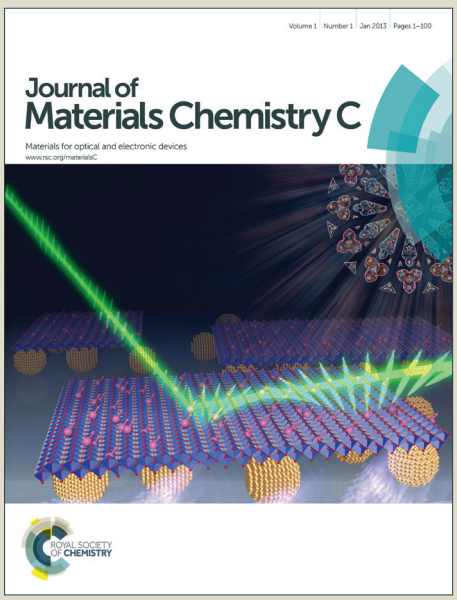

ROYAL SOCIETY OF CHEMISTRY

www.rsc.org/materialsC

Cite this: DOI: 10.1039/c0xx00000x

www.rsc.org/xxxxxx

ARTICLE TYPE

Fast fabrication of transparent and multi-luminescent TEMPO-oxidized nanofibrillated cellulose nanopaper functionalized with lanthanide complexes

Miao Miao,[a] Jingpeng Zhao,[a] Xin Feng,*[a] Yang Cao,[c] Shaomei Cao,[a] Yafei Zhao,[a] Xiaoqian Ge,[a] Lining Sun,*[a] Liyi Shi[a,b] and Jianhui Fang*[b]

Received (in XXX, XXX) Xth XXXXXXXXX 20XX, Accepted Xth XXXXXXXXX 20XX
DOI: 10.1039/b000000x

We first designed an easy-to-fabricate multi-luminescent nanopaper with high transparency through grafting lanthanide complexes [$Eu(dbm)_3(H_2O)_2$, $Sm(dbm)_3(H_2O)_2$, $Tb(tfacac)_3(H_2O)_2$] on TEMPO mediated oxidized nanofibrillated cellulose (ONFC). The lanthanide complex functionalized ONFC nanopaper (Ln-ONFC nanopaper, Ln = Eu, Sm, Tb) with uniform luminescence was rapidly fabricated after solvent exchange using a press-controlled extrusion papermaking method. The new TEMPO-induced carboxyl groups on the surface of ONFC provided the possibility to participate in the coordination with lanthanide ions and then to construct heterogeneous network architectures. The fluorescent properties of Ln-ONFC hybrid nanopaper were significantly influenced by the amount of lanthanide complexes and the solvent medium during the extrusion. Based on the simple manipulation and mild condition, highly transparent NFC template fulfilled a soft matrix and afforded the high thermal stability and excellent luminescent properties of the Ln-ONFC nanopaper, which would yield an ever increasing potential to supersede petroleum-based materials for diverse applications.

1. Introduction

Traditionally, petroleum-based polymers have been extensively used due to their simple processing and low manufacturing costs[1]. However, most of them have larger coefficients of thermal expansion (CTE) than those of functional inorganic deposited materials, resulting in invalidation of flexible devices under the condition of repeated bending or large changes in temperature. Nowadays, with ever increasing consciousness for global environment and energy sources, the utilization of eco-friendly and renewable native biopolymers are attracting extensive attentions. Optical transparent nanopaper based on nanofibrillated cellulose (NFC) is emerging as a novel, environmentally friendly, biodegradable and renewable material, which could be the perfect candidates for plastic substrates in the future production of flexible electronics, such as solar cells, radio frequency identification (RFID) antennas, touch screens, chemical and biological sensors, organic field-effect transistors (OFETs) and a myriad of new flexible circuit technologies[2-7]. The biobased composition of NFC nanopaper is similar with that of traditional paper except that NFC nanopaper is made of nanocrystalline cellulose with smaller diameter and higher crystallinity. As a result, NFC nanopaper exhibits excellent optical transmittance compared to regular cellulose paper. Furthermore, the low CTE (12-28.5 $ppmK^{-1}$), high tensile strength, enhanced printability and recyclability make it easy to process in high temperature than plastic substrates[8-10].

Luminescent materials based on trivalent lanthanide ions have attracted much attention during the last decade. The luminescent lanthanide complexes display unique properties including sharp emission peaks, high colour purity, long lifetime and relative low toxicity[11-14], making them promising in the fabrication of new type of anti–counterfeiting facilities, sensor systems and ion probes applications. NFC is an ideal building block to host a range of guest materials for NFC-based flexible matrices. The functionalized NFC hybrid nanopaper has attracted tremendous interest combined with the exciting synergetic characteristics including conductivity, fluorescence, magnetism, fire retardancy and gas barrier functions[4-7,15-18]. Recently, the synthesis and luminescent properties of inorganic quantum dots/cellulose, rare-earth complex/cellulose and their derivatives nanocomposites have been reported[19-23].

However, two issues that need to be addressed for the fast fabrication of NFC hybrid nanopaper with homogenous network architectures still remain. First, to incorporate the lanthanide complexes into the soft matrix, a problem often encountered by physical doping method is the nonhomogeneous distribution of the complexes, which always leads to unavoidable agglomeration and a decrease of the luminescence intensity. As an alternative, by covalent linking of the complexes to the host matrix, a more homogeneous distribution of the lanthanide complex in the NFC network gives the possibility to achieve hybrid nanopaper. Secondly, for fabricating NFC nanopaper, the difficulty is the extremely slow dewatering because of the high water binding capacity of NFC[1,24,25]. Traditionally, NFC nanopaper prepared by using suspension-casting, water evaporation, and hot pressing to remove the excessive water is extremely time-consuming, the procedures usually require from several hours to a few days and even longer with complicated manipulations[26-28]. Sehaqui et al. reported that flat nanopaper was prepared in about 1 h using a semiautomatic sheet former under vacuum[29]. Österberg et al. introduced an overpressure filtration for fast preparation of NFC

films in less than 1 h, but there was always about 40% loss of material during the filtration[1].

Herein, a facile and highly efficient approach has been attempted to fabricate transparent and multi-luminescent nanopaper by the well dispersed 2,2,6,6-Tetramethylpiperidinooxy (TEMPO) mediated oxidized NFC (ONFC) grafting with lanthanide complexes [$Eu(dbm)_3(H_2O)_2$, $Sm(dbm)_3(H_2O)_2$, $Tb(tfacac)_3(H_2O)_2$] by using a pressure-controlled extrusion paper–making process. ONFC aqueous suspensions were treated with ethanol exchange to form homogeneous solution with lanthanide complexes. The carboxyl groups on the surface of ONFC participate in the covalent coupling process with lanthanide ions to form heterogeneous network architectures. The obtained Ln-ONFC hybrid nanopaper combines the advantages of both lanthanide complexes and NFC nanopaper and exhibits synergetic properties. To the best of our knowledge, it is the first time to synthesize lanthanide complex functionalized ONFC by coupling reaction for easy fabrication of multi-luminescent nanopaper in less than 15 min without adopting additional constraint clamping under vacuum to prevent wrinkling. Furthermore, the whole procedure is simple operation, mild reaction condition and being environmentally-friendly.

2. Experimental section

2.1 Reagents and materials

1,1,1-trifluoroacetylacetone (Htfacac, 99%, Alfa Aesar), dibenzoylmethane (Hdbm, AR, Aladin) were used without further purification. Samarium oxide (Sm_2O_3, 99.99%), europium oxide (Eu_2O_3, 99.99%), and terbium oxide (Tb_4O_7, 99.99%) were bought from Sigma-Aldrich. Hydrated $LnCl_3$ salts (Ln = Eu, Sm, Tb) were obtained by dissolving Ln_2O_3 (Ln = Eu, Sm) or Tb_4O_7 in hydrochloric acid. The resulting solutions were evaporated with heating; the residues were dissolved in the distilled water. 2,2,6,6-tetramethyl-piperidinyl-1-oxyl (TEMPO, 98%) was purchased from Sigma Aldrich. Ethanol (AR, 95%), sodium bromide (NaBr, AR), sodium hypochlorite (NaClO) were purchased from Sinopharm Chemical Reagent Co., Ltd (China) without further purification.

NFC aqueous suspensions were extracted after the chemical cleavage of the amorphous region of dealginate kelp residues by a high-pressure homogenization process (D–3L, PhD Technology LLC, USA).

The lanthanide complexes ($Eu(dbm)_3(H_2O)_2$, $Sm(dbm)_3(H_2O)_2$, $Tb(tfacac)_3(H_2O)_2$) were synthesized according to the previously reported work[30, 31].

2.2 Preparation of TEMPO-mediated oxidized nanofibrillated cellulose (ONFC) ethanol suspension

ONFC was prepared according to a previously procedure described by Lin et al.[32]. This method used TEMPO as a catalyst with the primary oxidant such as hypochlorite to oxidize the hydroxyl groups on the surface of NFC. Briefly, NFC aqueous suspensions were firstly treated by ultrasonic dispersion for 15 min. And then the solution of TEMPO and NaBr in a given ratio was added successively. The oxidizing reaction started by adding a certain amount of NaClO solution to the mixed dispersion, and pH value was maintained at 10 by adding NaOH solution. After 3 h, the pH was adjusted to 7 with hydrochloric acid addition. Finally, the ONFC ethanol suspensions were prepared using a conventional solvent exchange process. ONFC aqueous suspensions were sonicated and centrifuged to remove the supernatant, and then the obtained filter cake were dispersed in ethanol with sonication and filtered again. This process was repeated for five times and finally the filter cake was redispersed in ethanol to form 0.03 wt% colloidal suspensions.

2.3 Preparation of lanthanide complex grafted TEMPO-mediated oxidized nanofibrillated cellulose (Ln-ONFC) ethanol suspensions

Different amount (5, 7.5, 10, 12 mg) of lanthanide complex $LnL_3(H_2O)_2$ (L = dbm, Ln = Eu, Sm; L = tfacac, Ln = Tb) was added in the 50 mL 0.03 wt% ONFC ethanol suspensions under stirring for 30 min, respectively. The resulting luminescent ONFC (Ln-ONFC, Ln = Eu, Sm, Tb) suspensions were obtained by using the coupling reaction between $LnL_3(H_2O)_2$ and the carboxylate groups (–COONa) of ONFC.

2.4 Preparation of luminescent Ln-ONFC hybrid nanopaper

The schematic diagram of the formation of Ln-ONFC nanopaper was shown in Scheme 1. The luminescent Ln-ONFC ethanol suspensions were poured into the extruder (NanoAble-150, PhD Technology LLC, USA) to remove ethanol with controlled pressure of 0.6 MPa under N_2 gas, and nanopaper was formed on the filter membrane (PC, nuclepore track-etch membrane, pore size 100 nm, Whatman, UK) in less than 15 min. Then the nanopaper was peeled off and sandwiched between two pieces of glass dried at ambient atmospheres. Subsequently, transparent, flexible, and luminescent Ln-ONFC hybrid nanopaper with 45 mm in diameter and 30 μm in thickness was finally fabricated.

2.5 Preparation of Eu-ONFC-H_2O nanopaper

As the comparison, Eu-ONFC-H_2O nanopaper was prepared with aqueous suspensions other than ethanol suspensions by using the similar extrusion paper–making method.

2.6 Preparation of pure NFC and ONFC nanopaper

As the comparison, pure NFC nanopaper was synthesized without TEMPO oxidation and the lanthanide complexes addition, and pure ONFC nanopaper was also synthesized without the lanthanide complexes addition by using the similar extrusion paper–making method.

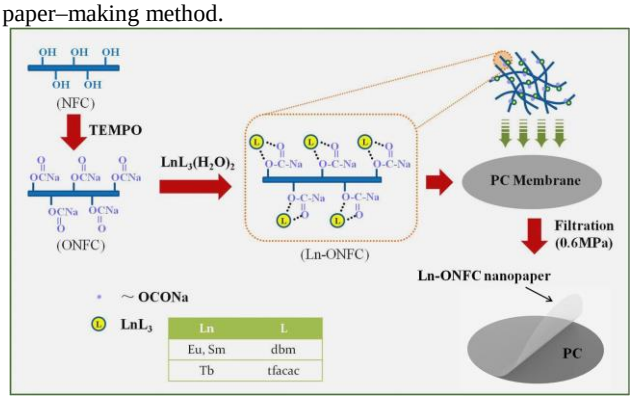

Scheme 1 Schematic diagram of the formation of Ln-ONFC hybrid nanopaper.

2.7 Characterization

The structure was characterized through Fourier transform infrared spectroscopy (FTIR, AVATAR370, USA) with the spectral width ranging from 4000 to 400 cm^{-1} by grinding KBr as transparent pellets. Surface morphologies were examined by scanning electron microscopy (SEM, JSM-6700F, JEOL, Japan). The optical properties were measured by UV–Vis spectrophotometer (UV-2501PC, Shimadzu, Japan). The excitation and emission spectra were measured with Spectrofluorophotometer (RF-5301PC, Shimadzu, Japan; FLS-920, Edinburgh, UK). The thermal stability was investigated by a thermogravimetric analyzer (TGA, STA409PC, Netzsch, Germany). The thickness of the samples was measured three times with a paper thickness meter (PT-4A, China).

3. Results and discussion

The FTIR spectra of pure NFC nanopaper, ONFC nanopaper and Eu-ONFC nanopaper are shown in Figure 1. The characteristic signals located at 3417 cm^{-1} and 2901 cm^{-1} are attributed to stretching vibration of −OH groups and stretching vibrations of C−H, respectively[33]. Upon the TEMPO oxidation, the important change for ONFC and Eu-ONFC is the appearance of the carboxyl groups (C=O) resulting from the surface sodium carboxylate groups (−COONa). In the spectrum of ONFC nanopaper, the carboxyl groups (C=O) was hardly observed due to the interference of the absorbed water band (1636 cm^{-1})[32]. To clearly observe the change from the oxidation, ONFC nanopaper was treated by HCl solution according to the previous literature[32]. −COONa was converted to acidic form –COOH under a procedure of ion exchange. The carboxyl groups (C=O) stretching vibration at 1734 cm^{-1} is clearly shown ascribed to –COOH. After the immobilization of $Eu(dbm)_3(H_2O)_2$ on ONFC, the new peak located at 1612 cm^{-1} was assigned to the strong stretching vibration of carboxylate[32], suggesting the coupling reaction between ONFC and $Eu(dbm)_3(H_2O)_2$[34]. The FT-IR spectra of other Ln-ONFC (Ln = Tb, Sm) nanopapers are very similar to that of Eu-ONFC. Therefore, the FTIR results demonstrated that the $LnL_3(H_2O)_2$ (L = dbm, Ln = Eu, Sm; L = tfacac, Ln = Tb) have been covalently bonded with ONFC, resulting in the formation of Ln-ONFC nanopaper.

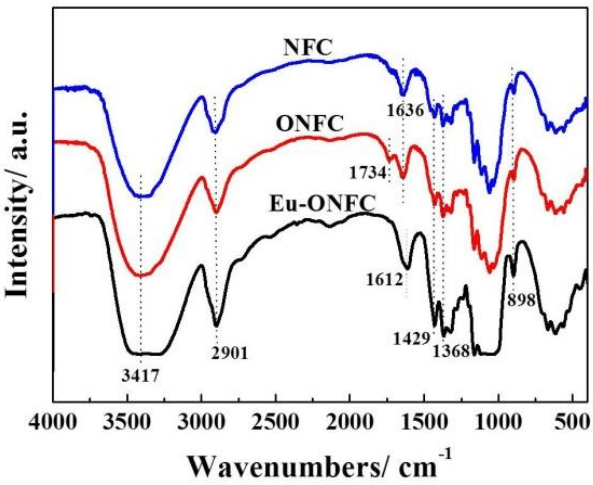

Fig. 1 FTIR spectra of pure NFC nanopaper, ONFC nanopaper and Eu-ONFC nanopaper.

The luminescence properties of Eu-ONFC nanopaper were investigated by fluorescence spectra. Fig. 2 shows the excitation and emission spectra of Eu-ONFC nanopaper. The excitation spectrum was obtained by monitoring the strongest emission of the Eu^{3+} at 616 nm. A broad band in UV/visible region ranging from 250 to 400 nm can be observed, which is attributed to the absorption of organic ligands (dbm and ONFC). Under the excitation at 336 nm, the characteristic emission bands at 579 nm, 591 nm, 616 nm, 650nm and 697 nm of Eu-ONFC nanopaper can be assigned to the $^5D_0 \rightarrow {}^7F_J$ (J =0, 1, 2, 3 and 4) transitions of Eu^{3+} ion. The $^5D_0 \rightarrow {}^7F_2$ transition at 616 nm is the strongest emission, which is an induced electric dipole transition and is responsible for the brilliant red emission of Eu-ONFC nanopaper[35]. It can be deduced that the dbm and ONFC ligands are able to transfer the absorbed UV energy to the Eu^{3+} ion via the antenna effect and the corresponding Eu complexes are formed between Eu^{3+} ion and the ligands in Eu-ONFC nanopaper. The emission spectra of Eu-ONFC nanopaper added with different amount of $Eu(dbm)_3(H_2O)_2$ complexes (0-12 mg) is shown in Fig. S1. It can be observed that the emission intensity gradually enhances with the amount of $Eu(dbm)_3(H_2O)_2$ complexes increasing. Then it is reasonable to deduce that, in a qualitatively way, no quenching effects were detected with increasing the amount of lanthanide complexes from 0 to 12 mg, as the experimental conditions (such as excitation power and detection slits) were kept constant during the entire set of measurements.

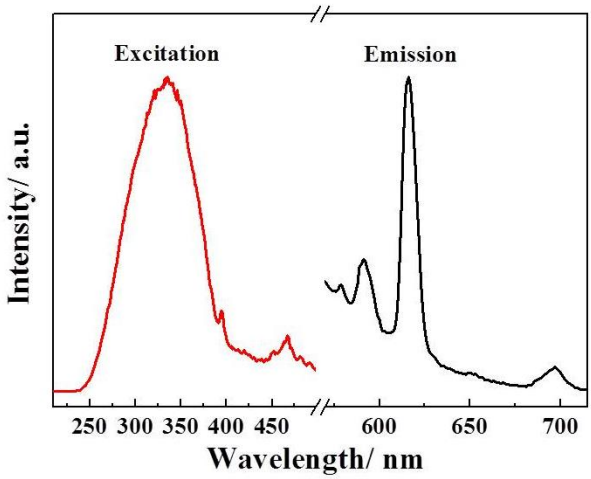

Fig. 2 Excitation and emission spectra of Eu-ONFC nanopaper with 10 mg $Eu(dbm)_3(H_2O)_2$.

The distribution and morphologies of lanthanide complex would play a critical role on the optical transmittance and luminescence properties of the nanopaper that contains with the lanthanide complex[6,19,36]. The SEM images of luminescent Eu-ONFC nanopaper with different dosages of 5 mg, 7.5 mg, 10 mg and 12 mg $Eu(dbm)_3(H_2O)_2$ are shown in Fig. 3, respectively. It can be noted that all the Eu-ONFC nanopaper exhibited a compact and uniform fibrous network structure assembled with NFC template. With the increase of $Eu(dbm)_3(H_2O)_2$ concentration to 10 mg in the initial ethanol suspensions, the relative smooth surface of Eu-ONFC nanopaper can be preserved (Fig. 3a-c). However, the increasing $Eu(dbm)_3(H_2O)_2$ amount (12 mg) would result in the rough and lumpy surface of nanopaper inevitably (Fig. S2). In addition, with the amount of

$Eu(dbm)_3(H_2O)_2$ being about 10 mg, the uniform red emission can be obtained under excitation with UV light at 365 nm (inset of Fig. 3c). The increase of $Eu(dbm)_3(H_2O)_2$ concentration will result in the reduction of uniformity of heterogeneous network architectures of Eu-ONFC nanopaper. The lower loading of $Eu(dbm)_3(H_2O)_2$ will be followed with a relatively decreasing luminescent intensity of the Eu-ONFC nanopaper. Taking into account the results mentioned above, an optimum lanthanide complex amount (10 mg) can be employed to synthesize the following Ln-ONFC (Ln = Sm, Tb) nanopaper with a high loading of lanthanide complex yet a uniform heterogeneous network architecture.

When the solvent of ethanol was replaced by H_2O during the synthesis process of nanopaper, the resulting Eu-ONFC-H_2O nanopaper (with 10 mg $Eu(dbm)_3(H_2O)_2$) shows a highly rough surface (Fig. 3d) and non uniform luminescence (inset of Fig. 3d). Therefore, the kinds of solvent play important role in the synthesis of uniform luminescent nanopaper. For the Eu-ONFC-H_2O nanopaper, it may be due to the hydrophobic property of the lanthanide complex $Eu(dbm)_3(H_2O)_2$ in aqueous medium causing an inadequate linking and poor compatibility with ONFC. The coordination of $Eu(dbm)_3(H_2O)_2$ and ONFC in water leads to inhomogeneous distribution and aggregation of Eu complex, resulting in the irregular surface and non uniform luminescence of Eu-ONFC-H_2O nanopaper.

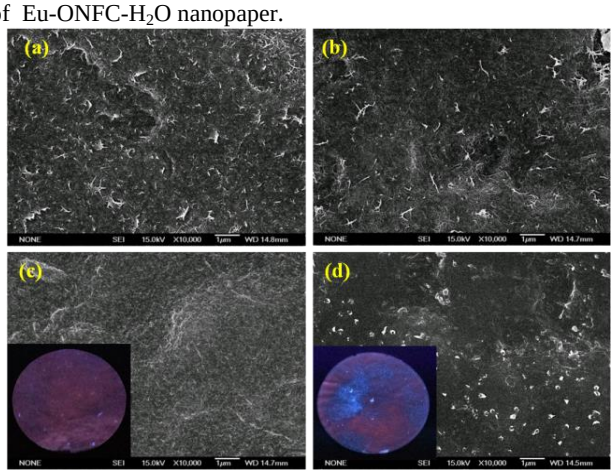

Fig. 3 Typical SEM images of the luminescent Eu-ONFC nanopaper with different $Eu(dbm)_3(H_2O)_2$ contents: 5 mg (a), 7.5 mg (b) and 10 mg (c). SEM image of Eu-ONFC-H_2O nanopaper prepared by H_2O as solvent with optimal dosage of 10 mg (d). Insets in c and d: the emission photos of nanopaper under excitation with UV light (365 nm).

The optical transparency of nanopaper was investigated, as shown in Fig 4. As the diameters of the NFC and ONFC are in the range of 10-20 nm (Fig. S3), the light scattering effect is significantly reduced and most of the light propagates through the nanopaper[6]. So both ONFC and Eu-ONFC nanopaper display very high transmittance in comparison with the previously reported nanopaper[29,37]. Compared with ONFC nanopaper, the light transmittance of Eu-ONFC nanopaper decreased slightly from 94% to 84% at the wavelength of 400 nm, which is probably attributed to the light absorption of lanthanide complex and the light scattering of relative rough nanopaper. The transparent and foldable properties of the resulting Eu-ONFC nanopaper can be further demonstrated from the inset pictures. Fig. 4a shows the picture of Eu-ONFC nanopaper with close contact to a flower, displaying the high optical transparency. As shown in Fig. 4b, the Eu-ONFC nanopaper is as foldable as conventional paper. Through the transparent and luminescent Eu-ONFC nanopaper, the school emblem of Shanghai University on the background can be clearly identified. While the school emblem behind the folded part becomes fuzzily, it is attributed to the large light scattering effect of the incident light[6,38]. Therefore, the flexibility, unique optical transparency and haze of luminescent Eu-ONFC nanopaper would expand their usage for applications in anti-glare, wearability and portability, etc.

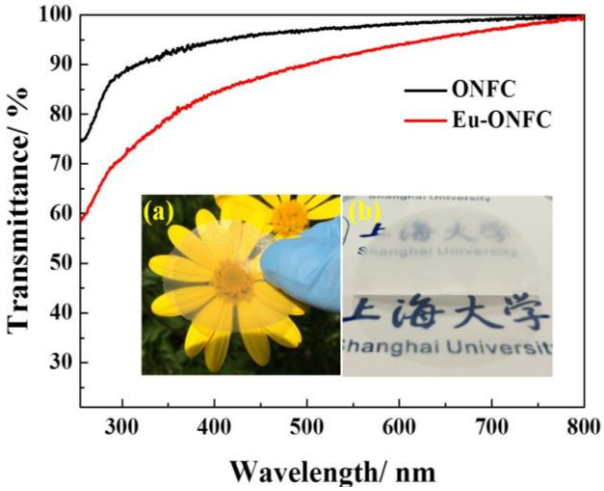

Fig. 4 Optical transmittance curves of ONFC nanopaper and Eu-ONFC nanopaper with 10 mg $Eu(dbm)_3(H_2O)_2$. Inset: the pictures of transparent (a) and foldable (b) Eu-ONFC nanopaper.

Encouraged by the excellent transparency and luminescent property of Eu-ONFC nanopaper and the efficient synthetic method, Sm-ONFC nanopaper and Tb-ONFC nanopaper were also synthesized by using the similar method except that $Eu(dbm)_3(H_2O)_2$ was replaced by $Sm(dbm)_3(H_2O)_2$ and $Tb(tfacac)_3(H_2O)_2$ with optimal dosage of 10 mg, respectively. Fig. 5 reveals the SEM morphologies of Sm-ONFC nanopaper and Tb-ONFC nanopaper. It can be noted that both Sm-ONFC nanopaper and Tb-ONFC nanopaper show smooth surface morphologies with uniform distribution of numerous interconnected ONFC, which are similar with that of Eu-ONFC nanopaper. The result indicates that different lanthanide complexes have no obvious effect on the morphology of Ln-ONFC nanopaper.

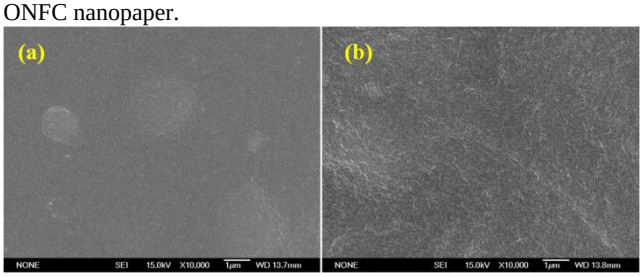

Fig. 5 Typical SEM morphologies of the Sm-ONFC nanopaper (a) and Tb-ONFC nanopaper (b).

The excitation and emission spectra of Sm-ONFC nanopaper and Tb-ONFC nanopaper are displayed in Fig. 6, respectively. As shown in Fig. 6a, the excitation spectrum of Sm-ONFC nanopaper, measured by monitoring the strongest emission of the

Sm^{3+} at 650 nm, displays a broad band ranging from 320 to 450 nm, attributed to the absorption of the ligands. In the visible emission spectrum of Sm-ONFC nanopaper (λ_{ex} = 380 nm), the strongest emission at 650 nm can be observed, which is due to the $^4G_{5/2} \rightarrow {}^6H_{9/2}$ transition of Sm^{3+} ion[14]. It is found that Sm-ONFC nanopaper displays orange luminescence upon UV excitation at 365 nm (inset in Fig. 6a). The excitation spectrum of Tb-ONFC nanopaper (Fig. 6b) was obtained by monitoring the strongest emission of Tb^{3+} ion (λ_{em} = 545 nm). The spectrum exhibits a broad band in the UV region, which is due to the absorption of the tfacac and ONFC ligands. Upon excitation at 304 nm, the emission spectrum of Tb-ONFC nanopaper shows the characteristic luminescence of Tb^{3+} ion, located at 488 nm ($^5D_4 \rightarrow {}^7F_6$), 545 nm ($^5D_4 \rightarrow {}^7F_5$), and 582 nm ($^5D_4 \rightarrow {}^7F_4$), in which $^5D_4 \rightarrow {}^7F_5$ transition is the most prominent one. Upon UV light illumination (254 nm), Tb-ONFC nanopaper displays green luminescence, which can be easily detected by naked eye (inset in Fig. 6b)[39]. As described above, the visible luminescence of lanthanide ions was obtained in the corresponding Ln-ONFC nanopaper (Ln = Eu, Sm, Tb) following excitation of the absorption of organic ligands, respectively. Thus, it is obvious that the intramolecular energy transfer does happen between the ligands and the Ln^{3+} ions. Therefore, it is reasonable to conclude that the ternary lanthanide complexes are bonded to ONFC.

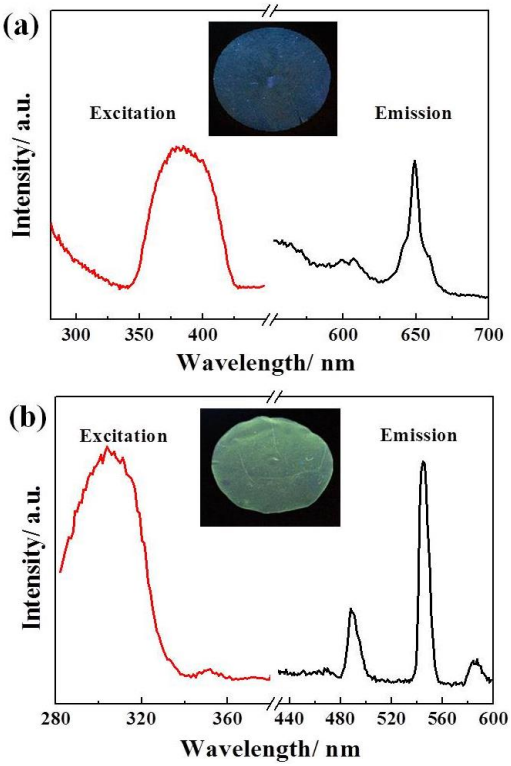

Fig. 6 Excitation and emission spectra of (a) Sm-ONFC nanopaper and (b) Tb-ONFC nanopaper. Inset: photos of Sm-ONFC nanopaper excited with UV light at 365 nm (a) and Tb-ONFC nanopaper excited with UV light at 254 nm (b).

The thermal stability of ONFC hybrid nanopaper was another important parameter to pave the way for a variety useful application as biopolymer substrates or inter-spacing layer. It has been demonstrated much lower CTE of nanopaper than glass and plastic[9,10], suggesting the better capability to tolerate large changes in temperature. The thermal stability of Ln-ONFC nanopaper (Ln = Eu, Sm, Tb) was investigated by TG analysis. The TG profiles of Ln-ONFC nanopaper are very similar, and Eu-ONFC nanopaper is given as representative. As shown in Fig. 7, TGA curves of ONFC nanopaper and Eu-ONFC nanopaper both exhibit three stages of weight loss. The first stage from the range of 20 ℃ to 220 ℃ with a small weight loss is due to the evaporation of water or decomposition of some micromolecule. At the second stage from 220 ℃ to 370 ℃, cellulose undergoes the processes of depolymerisation, dehydration and decomposition of glycoside units with the main weight loss of 57% for ONFC and 62% for Eu-ONFC, respectively. The third stage happens because of the degradation of charred residues to form gaseous products of low molecular weight. In the first two stages, the degradation temperature of Eu-ONFC nanopaper was very close to that of pure ONFC nanopaper, while a little difference can be observed in the third stage. Eu-ONFC nanopaper presents more carbonized residues than ONFC, which was probably related to the introduction of lanthanide complex acting as flame retardants. The excellent property of thermal stability for Ln-ONFC nanopaper gives the possibility to replace other film materials for a wide application.

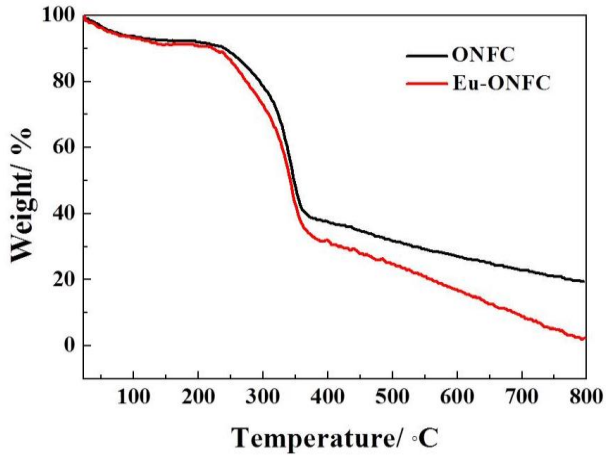

Fig. 7 TGA profiles of ONFC nanopaper and Eu-ONFC nanopaper with 10 mg $Eu(dbm)_3(H_2O)_2$.

In addition, a potential application of Ln-ONFC nanopaper used for security printing has been investigated. Quick response (QR) codes of about 25 mm×25 mm were directly printed on the surface of Tb-ONFC nanopaper using the colorless carbon dots (CD) aqueous solution as a printing ink. The CD aqueous solution obtained according to the previous report[40], has optimal excitation and emission peaks at 360 nm and 443 nm, respectively. Fig. 8 shows the digital pictures of the as-prepared Tb-ONFC nanopaper printed QR codes under daylight and UV light, respectively. It is obviously that Tb-ONFC nanopaper printed with QR codes maintains high transparency, and the QR codes are invisible under daylight (Fig. 8a), however, an anticipated blue luminescent QR codes appears under UV light excitation at 365 nm, as shown in Fig. 8b. Remarkably, when excited with UV light at 254 nm, green luminescent Tb-ONFC nanopaper and blue luminescent QR codes can be simultaneously observed. Therefore, the excellent "visible-invisible" and "UV-visible" properties of Ln-ONFC nanopaper printed with CD ink

can be easily applied for anti-counterfeiting and labelling fields[41], and the synergic features of transparency and multi-luminescence further strengthens the extensibility and fidelity in the multiple anti-counterfeiting technology for documents and products.

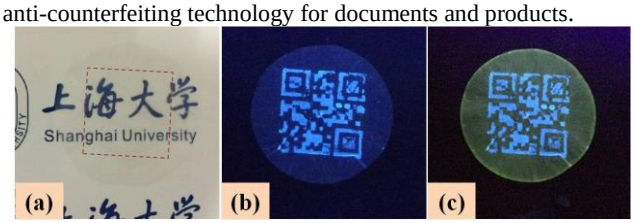

Fig. 8 The photos of Tb-ONFC nanopaper printed with QR codes by CD ink under daylight (a) and UV light at 365 nm (b) and 254 nm (c). The red dashed box of (a) marks the location of QR codes.

Conclusions

A fast press-controlled extrusion paper-making process has been used for three kinds of lanthanide complex functionalized ONFC hybrid nanopaper with high transparency for the first time. In the nanopaper-making process, a simple solvent exchange and subsequently fast extrusion procedure were included. Through the systematic and comparative study of the Eu-ONFC nanopaper with different amount of $Eu(dbm)_3(H_2O)_2$, the optimum lanthanide complex amount (10 mg) were selected as the candidate conditions for the preparation of Ln-ONFC (Ln = Eu, Sm, Tb) nanopaper. The three Ln-ONFC (Ln = Eu, Sm, Tb) nanopaper show good flexibility, unique optical transparency, and good thermal stability. Of importance is that after ligand-mediated excitation, the emission spectra of Ln-ONFC (Ln = Eu, Sm, Tb) nanopaper all show the characteristic luminescence of the corresponding lanthanide ions through the intramolecular energy transfer from the ligands to the lanthanide ions, indicating that the lanthanide complexes are formed and covalently linked to the ONFC network. The excellent properties and uniform luminescence (red for Eu-ONFC, orange for Sm-ONFC, and green for Tb-ONFC) of the Ln-ONFC nanopaper offer advantages including ease of synthesis and handling as well as potentially applications for anti-counterfeiting and labelling fields, and marking soft materials served for ID-card and credit card protection and other security applications.

Acknowledgements

This work was financially supported by the Science and Technology Commission of Shanghai Municipality (13ZR1415100, 15ZR1415100, 13JC1402700, 13NM1401101, 14520722200), the National Natural Science Foundation of China (Grant No 21231004), Innovation Program of Shanghai Municipal Education Commission (13ZZ073), Shanghai Foundation of Excellent Young University Teacher, and Shanghai Rising-Star Program (14QA1401800). The authors are also grateful to Instrumental Analysis & Research Center of Shanghai University.

Notes and references

[a] *Research Center of Nano Science and Technology, Shanghai University, Shanghai 200444, P. R. China. Fax: 86-21-66136038; Tel: 86-21-66137257; E-mail:fengxin@shu.edu.cn; lnsun@shu.edu.cn*

[b] *Department of Chemistry, Shanghai University, Shanghai 200444, P. R. China. Fax: 86-21-66132830; Tel: 86-21-66132830; E-mail:jhfang@shu.edu.cn*

[c] *School of Materials Sciences and Engineering, Shanghai University, Shanghai 200444, P. R. China.*

1 M. Österberg, J. Vartiainen, J. Lucenius, U. Hippi, J. Seppälä, R. Serimaa and J. Laine, *ACS Appl. Mater. Interfaces*, 2013, **5**, 4640.
2 H. L. Zhu, B. B. Narakathu, Z. Q. Fang, A. T. Aijazi, M. Joyce, M. Atashbar and L. Hu, *Nanoscale*, 2014, **6**, 9110.
3 T. S. Kim, S. I. Na, S. S. Kim, B. K. Yu, J. S. Yeo and D. Y. Kim, *Phys. Status Solidi (RRL)*, 2012, **6**, 13.
4 B. Wang and L. L. Kerr, *Sol. Energy Mater. Sol. Cells*, 2011, **95**, 2531.
5 M. C. Barr, J. A. Rowehl, R. R. Lunt, J. Xu, A. Wang, C. M. Boyce, S. G. Im, V. Bulović and K. K. Gleason, *Adv. Mater.*, 2011, **23**, 3500.
6 L. B. Hu, G. Y. Zheng, J. Yao, N. Liu, B. Weil, M. Eskilsson, E. Karabulut, Z. Ruan, S. Fan, J. T. Bloking, M. D. McGehee, L. Wågberg, and Y. Cui, *Energy Environ. Sci.*, 2013, **6**, 513.
7 J. W. Han, B. Kim, J. Li and M. Meyyappan, *J. Phys. Chem. C*, 2012, **116**, 22094.
8 H. L. Zhu, Z. Q. Fang, C. Preston, Y. Y. Li and L. B. Hu, *Energy Environ. Sci.*, 2014, **7**, 269.
9 R. J. Moon, A. Martini, J. Nairn, J. Simonsen and J. Youngblood, *Chem. Soc. Rev.*, 2011, **40**, 3941.
10 J. Huang, H. L. Zhu, Y. C. Chen, C. Preston, K. Rohrbach, J. Cumings and L. B. Hu, *ACS Nano*, 2013, **7**, 2106.
11 J. C. G. Bünzli and C. Piguet, *Chem. Soc. Rev.*, 2005, **34**, 1048.
12 J. C. G. Bünzli, *Acc. Chem. Res.*, 2006, **39**, 53.
13 L. N. Sun, W. P. Mai, S. Dang, Y. N. Qiu, W. Deng, L. Y. Shi, W. Yan and H. J. Zhang, *J Mater Chem*, 2012, **22**, 5121.
14 L. N. Sun, Y. N. Qiu, T. Liu, J. Z. Zhang, S. Dang, J. Feng, Z. J. Wang, H. J. Zhang and L. Y. Shi, *ACS Appl. Mater. Interfaces*, 2013, **5**, 9585.
15 H. L. Zhu, S. Parvinian, C. Preston, O. Vaaland, Z. C. Ruan and L. B, Hu, *Nanoscale*, 2013, **5**, 3787.
16 R. T. Olsson, M. A. S. Azizi Samir, G. Salazar-Alvarez, L. Belova, V. Ström, L. A. Berglund, O. Ikkala, J. Nogrés and U. W. Gedde, *Nat. Nanotechnol.*, 2010, **5**, 584.
17 A. D. Liu, A. Walther, O. Ikkala, L. Belova and L. A. Berglund, *Biomacromolecules*, 2011, **12**, 633.
18 J. P. Zhao, Z. W. Wei, X. Feng, M. Miao, L. N. Sun, S. M. Cao, L. Y. Shi and J. H. Fang, ACS Appl. Mater. Interfaces, 2014, **6**, 14945.
19 J. S. Huo, Y. H. Zheng, S. T. Pang, and Q. M. Wang, *Cellulose*, 2013, **20**, 841.
20 Z. H. Yang, S. Y. Chen, W. L. Hu, N. Yin, W. Zhang, C. Xiang and H. P. Wang, *Carbohyd. Polym.*, 2012, **88**, 173.
21 P. Kulpinski, A. Erdman, M. Namyslak, and J. D. Fidelus, *Cellulose*, 2012, **19**, 1259.
22 P. Kulpinski, M. Namyslak, T. Grzyb, and S. Lis, *Cellulose*, 2012, **19**, 1271.
23 H. Q. Wang, Z. Q. Shao, M. Bacher, F. Liebne, and T. Rosenau, *Cellulose* , 2013, **20**, 3007.
24 K. Junka, J. Guo, I. Filpponen, J. Laine, and O. J. Rojas, *Biomacromolecules*, 2014, **15**, 876.
25 W. Y. Huang , X. L. Ouyang, and L. J. Lee, *ACS Nano*, 2012, **6**, 10178.
26 M. Nogi, S. Iwamoto, A. N. Nakagaito, and H. Yano, *Adv. Mater.*, 2009, **21**, 1595.
27 T. Zimmermann, E. Pohler, and T. Geiger, *Adv. Eng. Mater.*, 2004, **6**, 754.
28 M. E. Malainine, M. Mahrouz, and A. Dufresne, *Compos. Sci. Technol.*, 2005, **65**, 1520.
29 H. Sehaqui, A. Liu, Q. Zhou and L. A. Berglund, *Biomacromolecules*, 2010, **11**, 2195.
30 L. N. Sun, H. J. Zhang, C. Y. Peng, J. B. Yu, Q. G. Meng, L. S. Fu, F. Y. Liu, and X. M. Guo, *J. Phys. Chem. B*, 2006, **110**, 7249.
31 C. R. D. Silva, J. Li, Z. P. Zheng, and L. R. Corrales, *J. Phys. Chem. A*, 2008, **112**, 4527.

32 N. Lin, C. Bruzzese, and A. Dufresne, *ACS Appl. Mater. Interfaces*, 2012, **4**, 4948.

33 C. Y. Chang, J. Peng, L. N. Zhang and D. W. Pang, *J. Mate. Chem.*, 2009, **19**, 7771.

34 Z. Zhou and Q. M. Wang, *Sensor. Actuat. B*, 2012, **173**, 833.

35 L. N. Sun, Z. J. Wang, J. Z. Zhang, J. Feng, J. L. Liu, Y. Zhao, and L. Y. Shi, *RSC Advances*, 2014**, 4,** 28481.

36 M. Surin, E. Hennebicq, C. Ego, D. Marsitzky, A. C. Grimsdale, K. Müllen, J. L. Brédas, R. Lazzaroni, and P. Leclère, Chem. Mater., 2004, 16, 994.

37 H. Sehaqui, N. E. Mushi, S. Morimune, M. Salajkova, T. Nishino and L. A. Berglund, *ACS Appl. Mater. Interfaces*, 2012, **4**, 1043.

38 Z. Q. Fang, H. L. Zhu, C. Preston, X. G. Han, Y. Y. Li, S. Lee, X.S. Chai, G. Chen and L.B. Hu, J. Mater. Chem. C , 2013, 1, 6191-6197

39 L. N. Sun, J. B. Yu, H. S. Peng, J. Z. Zhang, L. Y. Shi and O. S. Wolfbeis, *J Phys. Chem. C*, 2010, **114**, 12642.

40 S. Zhu, Q. Meng, L. Wang, J. Zhang, Y. Song, H. Jin, K. Zhang, H. Sun, H. Wang and B. Yang, *Angew. Chem.*, 2013, **125**, 4045.

41 S. S Liu, C. F Wang, C. X. Li, J. Wang, L. H. Mao and S. Chen, *J. Mater. Chem. C*, 2014, **2**, 6477.

Table of Contents

Transparent and multi-luminescent nanopaper was rapidly fabricated by TEMPO oxidized NFC grafting with lanthanide complexes via a pressured extrusion process.